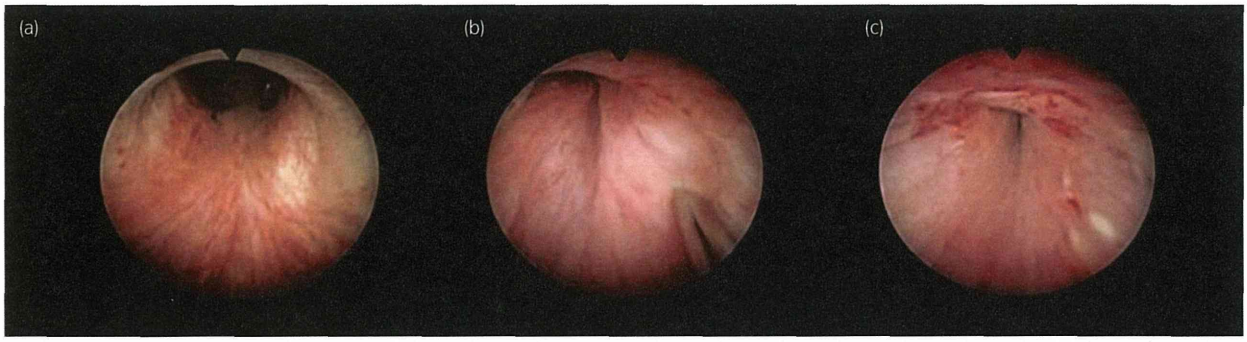

Fig. 1 Endoscopic findings during the procedures of periurethral injection of ADRC. The figure shows the findings in case 2. (a) Before injection, the urethral lumen at the region of the external urethral sphincter was open. (b) An 18-G needle punctured the urethra at 4 o'clock of the region of the external urethral sphincter (the arrow shows a puncture needle), (c) After completing the injection, the urethral lumen was closed and complete coaptation of the urethral mucosa was obtained.

A 22-Fr rigid nephroscope was used for injecting the processed ADRC cell suspension. Under endoscopic vision, a puncture needle was passed through the nephroscope into the urethra at the region of the external urethral sphincter. The puncture needle with a thickness of 18-G, length of 35 cm and graduated in centimeters was specially ordered. After puncturing the urethra at the region of the external urethral sphincter under endoscopic vision, the ADRC were injected. Initially, a 1-mL solution was injected at a depth of 5 mm into the rhabdosphincter at 5 and 7 o'clock positions. Subsequently, 20 mL of the formulation containing ADRC and adipose tissue was equally injected into the submucosal spaces at 4, 6 and 8 o'clock positions to facilitate complete coaptation of the urethral mucosa by the bulking effect. After the solution was injected, a 6-Fr urethral balloon catheter was placed and removed the following day.

Outcome measures

The amount of incontinence was evaluated by a 24-h pad test. The total daily leakage amount was calculated. The 24-h pad test was consecutively repeated for 4 days for each evaluation period. The subjective symptoms and QOL were evaluated using a validated disease-specific questionnaire – the ICIQ-SF.[18,19] In the ICIQ-SF, the therapeutic effects in terms of frequency of urinary incontinence (0–5 point scores), amount of leakage (0–6 point scores) and impact on everyday life (0–10 point scores) were examined, and the total score ranging from 0 to 21 points was calculated. A high score indicated an unfavorable condition. These parameters were assessed at baseline, and repeated 2, 4, 8, 12 and 24 weeks after treatment.

The urethral sphincter function was objectively assessed by measuring the urethral pressure profile using a urodynamic equipment (MMS, Enschede, The Netherlands). MUCP and FPL were measured at baseline, and 2, 12 and 24 weeks after treatment.

The blood flow to the area where ADRC were injected was assessed by contrast-enhanced transrectal ultrasonography by intravenously injecting perflubutane.[20] The morphological condition of the injected area was monitored by MRI.

Results

Liposuction from the abdomen was carried out without significant morbidity, and 250 mL of adipose tissues could be harvested. The isolated adipose tissue solution contained 3.3×10^7 ADRC (2.9×10^7 viable cells), 4.0×10^7 ADRC (3.8×10^7 viable cells) and 2.4×10^7 ADRC (2.2×10^7 viable cells) in cases 1, 2 and 3, respectively.

The urethral lumen at the region of the external urethral sphincter remained open, as observed by endoscopy, whereas the urethral lumen completely closed after the periurethral injection (Fig. 1).

Urinary incontinence improved within a few days after injection, deteriorated subsequently and progressively improved thereafter up to 6 months. At 6 months after injection, urinary incontinence improved in terms of leakage volume measured by a 24-h pad test in all cases, and disappeared in case 3 (Table 1). Assessment of subjective symptoms and QOL by the ICIQ-SF showed similar improvement (Table 2). Sphincteric function of the urethra was improved in all cases in terms of increased MUCP and FPL (Table 1).

After the urethral catheter was removed, all the patients could void without significant residual urine. None of the patients complained of voiding symptoms. Uroflowmetry did not show significant voiding dysfunction and an increase in the amount of residual urine (Table 1).

Enhanced ultrasonography showed a sequential increase in the blood flow to the area where ADRC were injected, which was maintained during the entire follow-up period (Fig. 2). MRI showed a bulking effect at the site of adipose

Table 1 Clinical outcome for objective findings

	Case	Baseline	2 weeks	4 weeks	8 weeks	12 weeks	16 weeks	24 weeks
24-h pad test (g)	1	108/134/127/120 (122.3)	59/100/80/122 (90.3)	80/115/90/58 (85.8)	99/110/95/102 (101.5)	68/70/88/119 (86.3)	98/21/33/104 (64.0)	34/45/60/63 (50.5)
during 4 days	2	30/35/66/67 (49.5)	23/54/38/44 (39.8)	47/29/22/23 (30.3)	43/25/23/27 (29.5)	43/25/23/27 (21.8)	14/10/13/13 (12.5)	12/11/11/12 (11.5)
(mean)	3	40/35/25/40 (35.0)	39/21/10/28 (24.5)	14/0/0/6 (5.0)	15/0/0/15 (7.5)	9/0/0/6 (3.8)	0/6/0/0 (1.5)	0/0/0/0 (0)
MUCP (cmH_2O)	1	40	59	–	–	52	–	53
	2	39	52	–	–	46	–	45
	3	28	25	–	–	43	–	40
FPL (mm)	1	20	20	–	–	25	–	24
	2	15	30	–	–	40	–	40
	3	14	20	–	–	32	–	28
Qmax	1	11.4	17.1	–	–	11.0	–	12.5
	2	37.0	18.9	–	–	7.5	–	19.3
	3	17.8	8.0	–	–	20.5	–	15.8
Postvoid	1	25	32	–	–	20	–	15
residue (mL)	2	50	60	–	–	10	–	50
	3	30	38	–	–	0	–	10

tissue injection, which persisted even at 12 weeks after injection (Fig. 3).

No significant adverse event was noted throughout the liposuction and ADRC injection procedures. No severe side-effects, such as pelvic pain, inflammation or de novo urgency, were observed after the operation in all cases during the postoperative follow up.

Discussion

ADRC have been successfully used in a variety of indications in humans, including the treatment of Crohn's disease-associated fistulas,[21] osteogenesis imperfecta,[22] and for breast augmentation and reconstruction after partial mastectomy.[23] Lin *et al.* reported the characterization of ADRC isolated with the Celution system in a basic investigation.[17] They showed by flow cytometry and CFU-F assays that the isolated cells from the Celution were composed of heterogeneous cell population including ASC, mature and progenitor endothelial cells, vascular smooth muscle cells, CD45+ hematopoietic cells, resident tissue macrophage/monocytes, pericytes, and preadipocytes and so on, containing ASC in 0.6–1.6% of all cell components. To explore the safety and feasibility of ADRC transplantation in patients with myocardial infarction, the first-in-man randomized controlled trial is currently in progress in the Netherlands.[15] Our cell therapy is the first attempt to use ADRC for treating SUI.

Before applying this new therapeutic technique to humans, we carried out several animal experiments using rats to confirm the effect of the periurethral injection of ASC on the urethral resistance and sequential changes of the injected rat ASC.[24] Cultured rat ASC were injected into the proximal urethra after bilateral transection of the pelvic nerves. Bladder leak point pressure was measured 4 weeks after injection of ASC, Gax-collagen or vehicle. Leak point pressure was significantly higher in the rats undergoing ASC injection as compared with those undergoing injection of collagen or vehicle. Additionally, GFP-expressing cultured ASC obtained from male GFP rats were injected into the urethra of female nude rats. Four weeks after the injection, anti-GFP antibody-positive cells were abundantly stained at the region of ASC injection. Furthermore, 12 weeks after the injection, alpha SMA-positive cells were stained in the merged distribution (70%) with the GFP expressing ASC, suggesting possible differentiation of ASC into smooth muscle cells. These preliminary animal experiments support the present clinical outcomes, such as progressive improvement of sphincteric function and incontinence. Dave *et al.* also reported the feasibility of ASC use as an improvement in leak point pressure and urethral function of SUI when animals were injected with ASC.[25] Recently, a variety of reports have suggested promising feasibility of ADRC and

Table 2 Clinical outcome for symptoms and QOL

	Case	Baseline	2 weeks	4 weeks	12 weeks	24 weeks
ICIQ-SF (frequency of leakage)	1	4	3	4	4	4
	2	5	5	5	4	4
	3	4	4	3	2	0
ICIQ-SF (amount of leakage)	1	4	4	4	3	3
	2	2	2	2	2	2
	3	4	2	2	2	0
ICIQ-SF (QOL)	1	6	6	3	3	3
	2	2	2	2	2	1
	3	4	3	3	3	0
ICIQ-SF (total score)	1	14	13	11	10	10
	2	9	9	9	8	7
	3	12	9	8	7	0

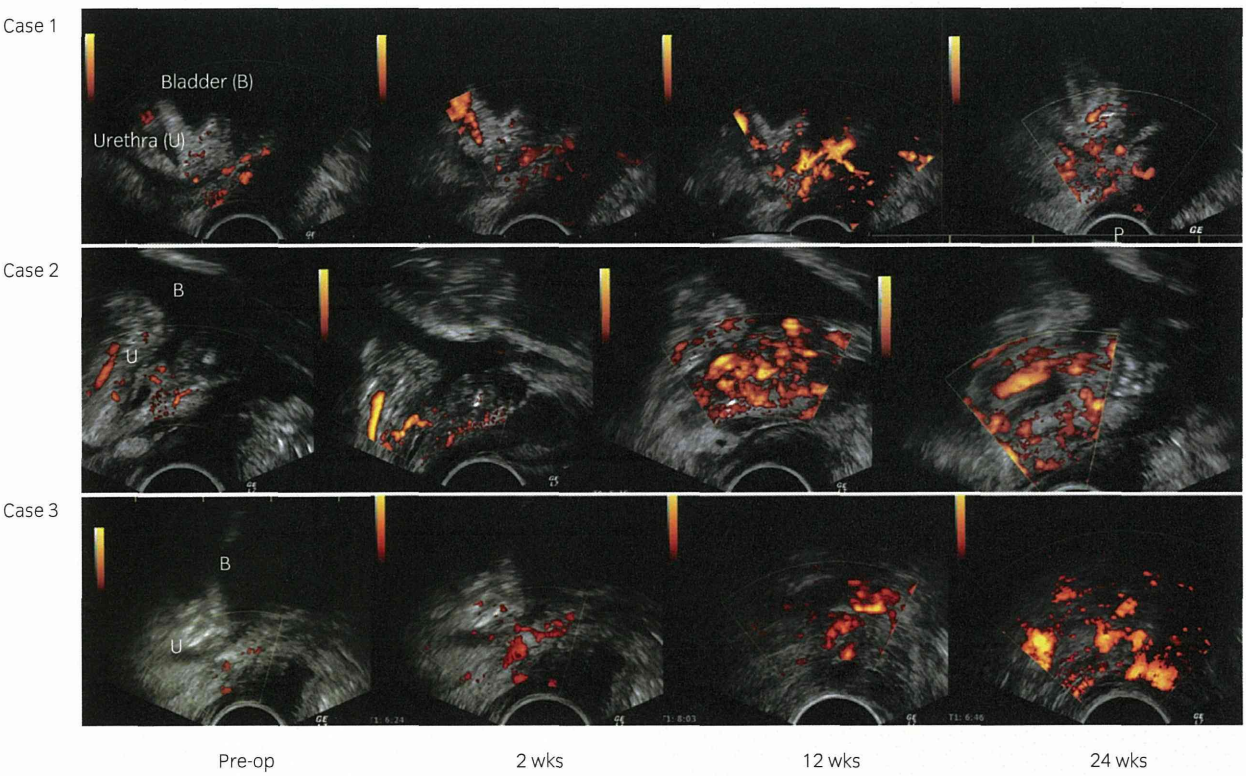

Fig. 2 Contrast-enhanced transrectal ultrasonography to assess the blood flow of the periurethral area after ADRC injection. The bladder and urethra was visualized as a sagittal section. The blood flow around the injected area visualized as orange color was progressively increased after the injection of ADRC up to 6 months in case 1, 2 and 3, showing a progressive increase of blood flow at the injection site.

ASC for regenerative treatment of SUI on an experimental level.[26,27]

Recently, cell therapy using autologous adult muscle-derived stem cells has been developed for treating SUI. A muscle biopsy sample was obtained from the upper arm and cultured to harvest two types of autologous muscle-derived cells: myoblasts and fibroblasts. The muscle-derived stem cells were injected transurethrally into the urethra. Carr *et al.* reported the outcomes of 1-year follow up of autologous muscle-derived stem cell injection to treat eight

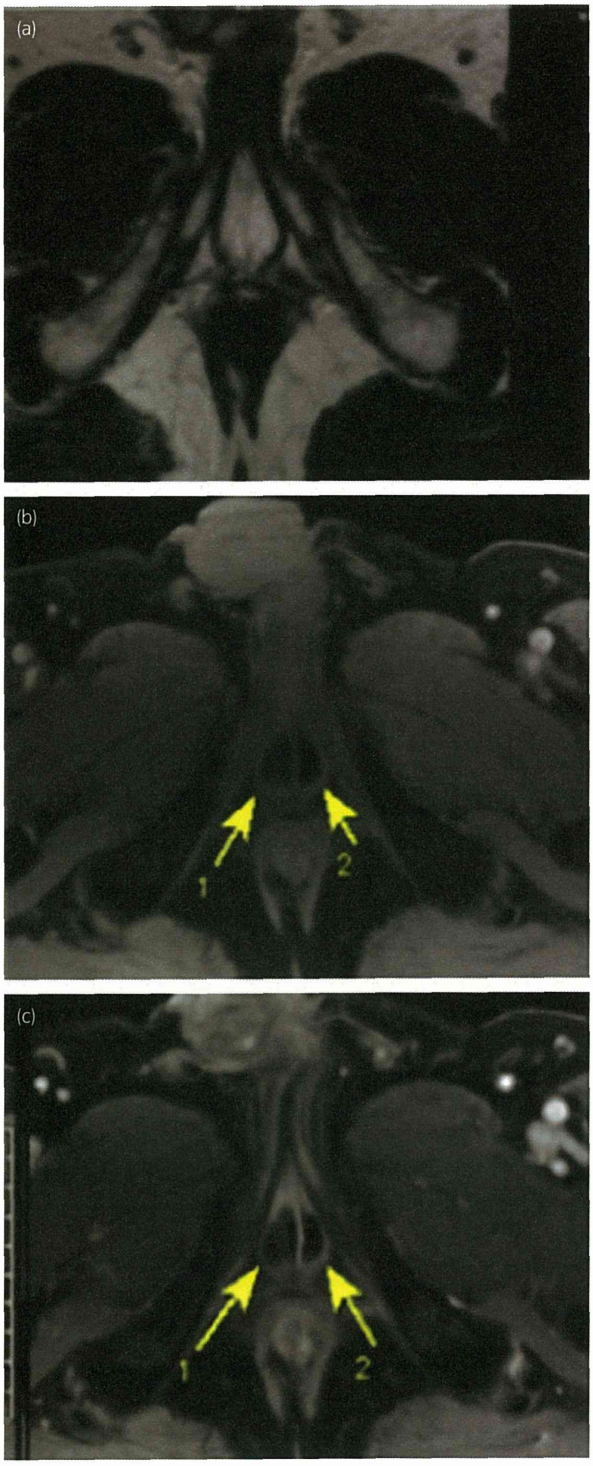

Fig. 3 Magnetic resonance imaging around the urethra before and after the ADRC injection. The urethra in case 1 was visualized as a cross-section on magnetic resonance imaging. (a) Before injection, (b) 4 days after injection and (c) 12 weeks after injection. The arrows demonstrate the adipose tissue injected with ADRC. There was no change in the volume of injected adipose tissue between 4 days and 12 weeks after injection.

women with stress incontinence.[28] With a mean follow-up period of 16.5 months, SUI was improved in five patients, with one achieving total continence, and no serious adverse events were noted. Our treatment strategy has an important advantage over the use of muscle-derived stem cells. Because adipose tissue contains abundant multipotent stem cells, as well as key mature cells and progenitor cells, therapeutic levels of regenerative cells can be obtained rapidly using the Celution system. In the present study, a therapeutically relevant number of cells could be isolated from each patient using this system. Unlike other cell therapy strategies, the treatment is all autologous, requires no cell culture and is carried out in the context of a single surgical procedure.

Periurethral injection of autologous fat was previously investigated in female patients with SUI; adipose tissue harvested from the abdomen was transurethrally injected into the submucosal layer under endoscopic vision. Although the injected adipose tissue could sustain a bulking effect, its efficacy was reported to be poor. In a randomized controlled trial that compared the efficacy of fat injection with that of a placebo injection (saline), the improvement rate after fat injection was poor (22%) at 3 months, with no difference to that produced by the placebo.[29] These findings suggested that mature adipocytes were unable to survive at the injected site.

In the periurethral injection of ADRC, it has been suspected that a variety of mechanisms are involved in the improvement of the sphincteric function. A similar clinical course in the present three cases implies the involvement of specific factors that can suggest the mechanisms underlying the treatment strategy: urinary incontinence improved within a week after injection, deteriorated subsequently, and progressively improved thereafter up to 24 weeks after the injection. A bulking effect produced by the injected adipose tissue fraction mixed with ADRC is of primary importance. The injected adipose tissue fraction, which was processed to isolate ADRC, contained 30% of lactated Ringer's solution. Absorption of the solution could be responsible for the temporary deterioration in the condition during the initial week. The ASC subpopulation in the ADRC might have contributed to the progressive improvement in sphincteric function, which was shown in terms of increased MUCP and FPL, as well as decreased frequency and amount of urinary incontinence. Persistent bulking effect indicates the survival and growth of the injected adipose tissue, which could also be attributed to the presence of ASC. ASC within the ADRC might differentiate into mature adipose tissue and, possibly, into contractile cells. Previous studies on rats showed that cultured ASC injected into the injured urethra differentiated into contractile cells with smooth muscle cell features.[30] Indirect effects of the injected ASC might also be responsible for the improvement. Cultured ASC are known to secrete a large number of angiogenesis-related cytokines.[17]

In the present study, increased blood flow to the injected area was suggested by ultrasonography. The increased blood flow seemed to be maintained throughout the follow-up period; this increased blood flow could be a result of the angiogenesis effect of the cytokines secreted by the injected ADRC. The increased blood flow might have a positive effect on the regeneration of the injected adipose tissue and impaired sphincteric function.

The present preliminary study showed that periurethral injection of the autologous ADRC is a safe and feasible treatment modality for stress urinary incontinence. We could establish the clinical course and obtained excellent short-time outcomes in the three initial cases undergoing this cell therapy; hence, we intend to increase the number of patients and confirm the long-term outcomes of this treatment modality.

Acknowledgment

This study was supported by a grant from Nagoya University Hospital.

Conflict of interest

None declared.

References

1 Carlson KV, Nitti VW. Prevention and management of incontinence following radical prostatectomy. *Urol. Clin. North Am.* 2001; **28**: 595–612.
2 Arai Y, Kaiho Y, Takei M *et al.* Burden of male stress urinary incontinence: a survey among urologists in Japan. *Int. J. Urol.* 2009; **16**: 915–17.
3 Okamura K, Nojiri Y, Seki N *et al.* Perioperative management of transurethral surgery for benign prostatic hyperplasia: a nationwide survey in Japan. *Int. J. Urol.* 2011; **18**: 304–11.
4 Crivellaro S, Singla A, Aggarwal N, Frea B, Kocjancic E. Adjustable continence therapy (ProACT) and bone anchored male sling: complication of two new treatments of post prostatectomy incontinence. *Int. J. Urol.* 2008; **15**: 910–14.
5 Fraser JK, Wulur I, Alfonso Z, Hedrick MH. Fat tissue. An underappreciated source of stem cells for biotechnology. *Trends Biotechnol.* 2006; **24**: 150–4.
6 Jiang Y, Jahagirdar BN, Reinhardt RL *et al.* Pluripotency of mesenchymal stem cells derived from adult marrow. *Nature* 2002; **418**: 41–9.
7 Nagaya N, Kanagawa K, Itoh T *et al.* Transplantation of mesenchymal stem cells improves cardiac function in a rat model of dilated cardiomyopathy. *Circulation* 2005; **112**: 1128–35.
8 Safford KM, Hicok KC, Safford SD *et al.* Neurogenic differentiation of murine and human adipose-derived stromal cells. *Biochem. Biophys. Res. Commun.* 2002; **294**: 371–9.
9 Gluckman E, Horowitz MM, Champlin RE *et al.* Bone marrow transplantation for severe aplastic anemia: influence of conditioning and graft-versus-host disease prophylaxis regimens on outcome. *Blood* 1992; **79**: 269–75.
10 Banfi A, Bianchi G, Galotto M, Cancedda R, Quarto R. Bone marrow stromal damage after chemo/radiotherapy: occurrence, consequences and possibilities of treatment. *Leuk. Lymphoma* 2001; **42**: 863–70.
11 Banfi A, Podesta M, Fazzuoli L *et al.* High-dose chemotherapy shows a dose-dependent toxicity to bone marrow osteoprogenitors: a mechanism for post-bone marrow transplantation osteopenia. *Cancer* 2001; **92**: 2419–28.
12 Zuk PA, Zhu M, Ashjian P *et al.* Human adipose tissue is a source of multipotent stem cells. *Mol. Biol. Cell* 2002; **13**: 4279–95.
13 Zuk PA, Zhu M, Mizuno H *et al.* Multilineage cells from human adipose tissue: implications for cell-based therapies. *Tissue Eng.* 2001; **7**: 211–28.
14 Halvorsen YD, Franklin D, Bond AL *et al.* Extracellular matrix mineralization and osteoblast gene expression by human adipose tissue-derived stromal cells. *Tissue Eng.* 2001; **7**: 729–41.
15 Rangappa S, Fen C, Lee EH, Bongso A, Sim EK. Transformation of adult mesenchymal stem cells isolated from the fatty tissue into cardiomyocytes. *Ann. Thorac. Surg.* 2003; **75**: 775–9.
16 Rehman J, Traktuev D, Li J *et al.* Secretion of angiogenic and antiapoptotic factors by human adipose stromal cells. *Circulation* 2004; **109**: 1292–8.
17 Lin K, Matsubara Y, Masuda Y *et al.* Charactrization of adipose tissue-derived cells isolated with the Celution TM system. *Cytotherapy* 2008; **10**: 417–26.
18 Avery K, Avery K, Donovan J *et al.* The ICIQ, a brief and robust measure for evaluating the symptoms and impact of urinary incontinence. *Neurourol. Urodyn.* 2004; **23**: 322–30.
19 Gotoh M, Homma Y, Funahashi Y, Matsukawa Y, Kato M. Psychometric validation of the Japanese version of the International Consultation on Incontinence Questionnaire-Short Form (ICIQ-SF). *Int. J. Urol.* 2009; **16**: 303–6.
20 Hagen EK, Magnusson A, Aksnes AK, Norberg M. Enhanced visualization of the normal prostate blood flow in young healthy volunteers using a new ultrasound contrast agent. *Acta Radiol.* 2001; **42**: 225–9.
21 Garcia-Olmo D, Garcia-Arranz M, Herreros D, Pascual I, Peiro C, Rodriguez-Montes JA. Phase I clinical trial of the treatment of Crohn's fistula by adipose mesenchymal stem cell transplantation. *Dis. Colon Rectum* 2005; **48**: 1416–23.
22 Horwitz EM, Gordon PL, Koo WK *et al.* Isolated allogenetic bone marrow-derived mesenchymal cells engraft and stimulate growth in children with osteogenesis imperfect: implications for cell therapy of bone. *Proc. Natl. Acad. Sci. U.S.A.* 2002; **99**: 8932–7.
23 Yoshimura K, Matsumoto D, Gonda K. A clinical trial of soft-tissue augmentation by lipoinjection with

adipose-derived stromal cells (ASC). International Fat Applied Technology Society (IFATS);Third Annual Meeting 2005; 9–10.
24 Watanabe T, Maruyama S, Yamamoto T *et al.* Increased urethral resistance by periuretahral injection of low serum cultured adipose-derived mesenchymal stromal cells in rats. *Int. J. Urol.* 2011; **18**: 659–66.
25 Dave DS, Gunther-Lopez V, Zhang R *et al.* Periurethral injection of autologous adipose-derived stem cells with hepatocyte growth factor-impregnated PLGA microsheres for treatment of stress incontinence in an animal model. *J. Urol.* 2008; **179** (Suppl): 568 (abstract).
26 Wu G, Song Y, Zheng X, Jiang Z. Adipose-derived stromal cell transplantation for treatment of stress urinary incontinence. *Tissue Cell* 2011; **43**: 246–53.
27 Roche R, Festy F, Fritel X. Stem cells for stress urinary incontinence: the adipose promise. *J. Cell. Mol. Med.* 2010; **14**: 135–42.
28 Carr LK, Steele D, Chancellor MB *et al.* 1-year follow-up of autologous muscle-derived stem cell injection pilot study to treat stress urinary incontinence. *Int. Urogynecol. J.* 2008; **19**: 881–3.
29 Lee PE, Kung RC, Drutz HP. Periurethral autologous fat injection as treatment for female stress urinary incontinence: a randomized double-blind controlled trial. *J. Urol.* 2001; **165**: 153–8.
30 Jack GS, Almeida FG, Zhang R, Alfonso ZC, Zuk PA, Rodriguez LV. Processed lipoaspirate cells for tissue engineering of the lower urinary tract: implications for the treatment of stress urinary incontinence and bladder reconstruction. *J. Urol.* 2005; **174**: 2041–5.

Editorial Comment

Editorial Comment from Dr Ishizuka to Periurethral injection of autologous adipose-derived regenerative cells for the treatment of male stress urinary incontinence: Report of three initial cases

Yamamoto *et al.* are to be congratulated for their well-structured and consequently evaluated work on incontinence therapy by adipose-derived regenerative cells (ADRC).[1] They were able to show that periurethral injection of the autologous ADRC is a safe and feasible treatment modality for male stress urinary incontinence.

We have already reported bone marrow-derived mesenchymal stem cell (MSC) transplantation into injured rat's or rabbit's urethral sphincter.[2,3] The problems of MSC are invasiveness of taking cells, culture time is required to obtain the sufficient therapeutic cell doses, and the necessity of checking the change of cell characters by cultures. As the authors mentioned in the introduction, adipose tissue contains multipotent cells that are similar to mesenchymal stem cells, and the abundance of stem cells in the adipose tissue is 100-fold higher than that in the bone marrow. So, ADRC is very attractive material to use for tissue engineering. However, even in animal models, there was almost no reports to compare the long-term efficacy and the safety between MSC and ADRC. Further study will be required.

The other difficulty in the clinical application is the selection of the patients. In this study, all patients had stress urinary incontinence after prostate surgery, so good informed consent is essential before carrying out this new therapy. A comparison also might be required between this therapy and an artificial sphincter.

There might be some problems to solve for this therapy. However, I believe that this report will be one of the landmarks in urology, regenerative medicine and tissue engineering.

Osamu Ishizuka M.D., Ph.D.
Department of Urology,
Shinshu University School of Medicine,
Matsumoto, Nagano, Japan
ishizuk@shinshu-u.ac.jp

DOI: 10.1111/j.1442-2042.2012.03011.x

Conflict of interest

None declared.

References

1 Yamamoto T, Gotoh M, Kato M *et al.* Periurethral injection of autologous adipose-derived regenerative cells for the treatment of male stress urinary incontinence: report of three initial cases. *Int. J. Urol.* 2012; **19**: 652–9.
2 Kinebuchi Y, Aizawa N, Imamura T *et al.* Autologous bone-marrow-derived mesenchymal stem cell transplantation into injured rat urethral sphincter. *Int. J. Urol.* 2010; **17**: 359–68.
3 Imamura T, Ishizuka O, Kinebuchi Y *et al.* Implantation of autologous bone marrow-derived cells reconstructs functional urethral sphincters in rabbits. *Tissue Eng. Part A* 2011; **17**: 1069–81.

Effect of Tamsulosin on Bladder Microcirculation in Rat Model of Bladder Outlet Obstruction Using Pencil Lens Charge-coupled Device Microscopy System

Shotarou Mine, Tokunori Yamamoto, Hideki Mizuno, Kuniyuki Endo, Yoshihisa Matsukawa, Yasuhito Funahashi, Masashi Kato, Ryohei Hattori, and Momokazu Gotoh

OBJECTIVE To determine the effect of tamsulosin hydrochloride on blood flow in the submucosal capillaries of the bladder (SCB) in a rat model of bladder outlet obstruction (BOO) using a pencil lens charge-coupled device microscopy system.

MATERIALS AND METHODS BOO was established in rats by partial ligature of the proximal urethra and was maintained for 2 weeks. Tamsulosin or saline (control) was subcutaneously administered using an osmotic pump for 2 weeks immediately after surgery. The pencil lens charge-coupled device microscopy system was used to visualize the bladder microcirculation and quantitatively assess the blood flow in the SCB by measuring the velocity of the blood flow at the base and dome of the bladder. The blood flow in the SCB of the sham-operated rats, control BOO rats, and tamsulosin-treated BOO rats was compared.

RESULTS The blood flow in the SCB was significantly greater at the base than at the dome of the bladder. The reduction in blood flow through the SCB at the base and dome of the bladder was more significant in the BOO rats than in the sham-operated rats. However, after pretreatment with tamsulosin, the BOO rats showed a significant increase in blood flow through the SCB at the base and dome of the bladder compared with that of the control rats. The pencil lens charge-coupled device microscopy system image showed that the BOO rats had chronic ischemic capillary injury, which was ameliorated by tamsulosin.

CONCLUSION The results of the present study suggest that tamsulosin hydrochloride protects the SCB from ischemic injury after BOO. UROLOGY ■: ■—■, 2012. © 2012 Elsevier Inc.

α_1-Adrenoceptor (AR) antagonists have been reported to improve, not only voiding symptoms, but also storage symptoms in patients with benign prostatic hyperplasia (BPH).[1] Tamsulosin hydrochloride is an α_1-AR antagonist widely used to treat the lower urinary tract symptoms associated with BPH. Tamsulosin has been reported to improve overactive bladder symptoms, such as urgency, frequency, and urgency incontinence associated with BPH, in addition to voiding symptoms.[2-4] Tamsulosin relieves functional prostatic obstruction and improves voiding symptoms by relaxing the smooth muscles of the urethra and prostate. However, the mechanism by which tamsulosin improves storage symptoms is not fully understood. The causes of storage dysfunction are multifactorial, but impaired blood flow in the bladder, which is attributable to bladder overdistension associated with lower urinary tract obstruction, is presumed to be an important factor.[4] We have developed the pencil lens charge-coupled device microscopy system (PLCMS) and established its usefulness in evaluating renal microcirculation.[5-7] The PLCMS can be used to visualize the microcirculation of the bladder and evaluate the blood flow at a submucosal capillary vessel. In our previous study, we showed that tamsulosin protects the submucosal capillaries of the rat bladder from ischemia-reperfusion injury.[8] In the present study, we used the PLCMS to investigate the effect of tamsulosin on the blood flow through the submucosal capillaries of the bladder (SCB) of a rat model of bladder outlet obstruction (BOO) and elucidate the mechanism by which α_1-AR antagonists improve storage symptoms.

Financial Disclosure: *The authors declare that they have no relevant financial interests.*

From the Department of Urology, Nagoya University Graduate School of Medicine, Nagoya, Japan

Reprint requests: Tokunori Yamamoto, M.D., Department of Urology, Nagoya University Graduate School of Medicine, 65 Tsurumai-cho, Nagoya 466-8550 Japan. E-mail: toku@med.nagoya-u.ac.jp

Submitted: July 11, 2011, accepted (with revisions): September 4, 2012

0090-4295/12/$36.00
http://dx.doi.org/10.1016/j.urology.2012.09.008

MATERIAL AND METHODS

The present study complied with the Regulations for Animal Experiments at the Nagoya University Graduate School of Medicine. We used the PLCMS (Krea Touch Scope, model 03-1, Krea Seiko, Tokyo, Japan) to the measure blood flow in the microcirculation of the bladder. The diameter of the conical lens at the tip of the PLCMS measurement probe is 1 mm, making it suitable for evaluation in small animals.[5-7] Using an adjustable micromanipulator with a precision of a few 10s of microns in the X, Y, and Z axes, we secured the tip of the conical lens from the external bladder wall, thereby allowing the blood flow in the SCB to be observed in real time. The PLCMS comprises a video recorder (DV-CAM, Sony, Tokyo, Japan), monitor, lighting apparatus, controller, camera, lighting guide, and a pencil lens. It has a spatial resolution of 0.86 μm and a time resolution of 33 ms. The distance between the probe and capillary was maintained at 30-50 μm by continuously adjusting the focus on a submucosal capillary during any physiological movement. The images of the microcirculation obtained using the pencil lens were recorded continuously on a videotape and digitized using a computer. The reflected image was captured and passed through a green filter and then converted to electrical signals using a charge-coupled device camera. Because red blood cells contain a red pigment, when the image is passed through a green filter, they appear black. The continuous images of the bladder microcirculation obtained using the PLCMS were processed, and the velocity at which the red blood cells travelled through the SCB was measured from sequences of the spatio-temporal images.[6]

In the present study, 28 female Wistar rats (Charles River Japan, Yokohama, Japan), aged 10 weeks, were used. BOO was established using a previously published method.[9] In brief, a polyethylene catheter (PE-20, Becton Dickinson, Franklin Lakes, NJ) with an outside diameter of 1.09 mm was inserted into the bladder by way of the urethra. The abdomen was opened through a midline incision, and the urinary bladder and urethra were exposed. Two silk sutures (5-0) were placed around the proximal urethra and tied with the intraluminal indwelling catheter in place. After removal of the catheter, the abdominal wall was sutured.[9] We previously reported the relationship between the bladder capacity and the velocity of the red blood cells in the submucosal capillary measured using the PLCMS.[9] The velocity started to decrease at >1 mL of bladder capacity. Thus, in the present study, we confirmed a bladder urine volume of <1 mL using ultrasonography at the velocity measurement.

The rats were divided into 3 groups. The sham-operated group (n = 9); the control group (n = 9), in which the rats were administered physiological saline; and the tamsulosin group (n = 10), in which the rats were administered tamsulosin. An Alzet osmotic pump (Alzet model 2002, Durect, Cupertino, CA) filled with tamsulosin hydrochloride (Astellas Pharma, Tokyo, Japan) or saline was inserted under the dorsal skin immediately after the BOO procedure. Tamsulosin hydrochloride or saline was continuously infused using this osmotic pump at a constant rate of 0.5 μL/h for 2 weeks. The concentration of tamsulosin solution (0.1 mg/mL) was calculated using the mean body weight of the rats at the start of drug administration and the following formula: X (mg/mL) = target dose (μg/kg/h) × 10^3 × mean body weight (kg)/0.5 (μL/h) × 10^3. The rats were allowed to recover and then housed for 2 weeks with ad libitum access to food and water. After 2 weeks, the changes in the blood flow through the SCB of the BOO model rats were measured using the PLCMS, and the data obtained for the base and dome of the bladders of the control and tamsulosin groups were compared.

Data are expressed as the mean ± standard deviation and were analyzed using Student's t test or Dunnett's multiple comparison test. The differences with $P < .05$ were regarded as significant.

RESULTS

Visualization of Bladder Microcirculation

The bladder microcirculation could be clearly visualized using the PLCMS (Fig. 1). We could measure the blood flow through the SCB at the base and dome of the bladder. Contrast was obtained by using the absorption values of the hemoglobin-containing erythrocytes; compared to the surrounding tissue, the erythrocytes appeared in negative contrast. Imaging of the endothelial or parenchymal cells was not possible. The SCB of the BOO rats was characterized by a manifestation of chronic ischemic capillary dysfunction with sporadic microvascular hemorrhage, scattered microvascular thrombosis indicating no blood flow, and irregular capillary flow (Fig. 1C,D). The SCB of the tamsulosin group showed improvement in sporadic microvascular hemorrhage, scattered microvascular thrombosis, and irregular capillary flow and became wider than the SCB of the BOO rats (Fig. 1E,F). Because of the rapid flow, individual erythrocytes could be discerned in the SCB of the tamsulosin group (Fig. 1E,F) and the sham group (Fig. 1A,B); however, only the flow of the erythrocytes could be observed in the sham group.

Effect of Tamsulosin on Blood Flow in Submucosal Capillaries of BOO Rats at Bladder Base and Dome

The mean bladder weight of the sham, control, and tamsulosin groups was 134.0 ± 8.6, 432.2 ± 32.0, and 400.2 ± 17.6 mg, respectively.

The blood flow through the submucosal capillaries at the bladder base (0.61 ± 0.09 mm/s) was significantly greater than that at the dome (0.43 ± 0.16 mm/s; $P < .05$) in sham-operated rats (Fig. 2). The reduction in blood flow through the submucosal capillaries at the base and dome of the bladder was more significant in the BOO rats (0.18 ± 0.09 mm/s at the base and 0.11 ± 0.06 mm/s at the dome; $P < .01$) than in the sham-operated rats. Tamsulosin administration (0.1 μg/kg/h) resulted in a more significant increase in blood flow through the submucosal capillaries in the bladder base (0.40 ± 0.08 mm/s) and dome (0.26 ± 0.04 mm/s) of the BOO rats than that in the control BOO rats ($P < .05$).

The mean systolic arterial blood pressure was 108 and 106 mm Hg in the control BOO and tamsulosin groups, respectively, with no significant difference.

COMMENT

Many investigators have described the use of laser Doppler blood flow (LDBF) for evaluating blood flow in

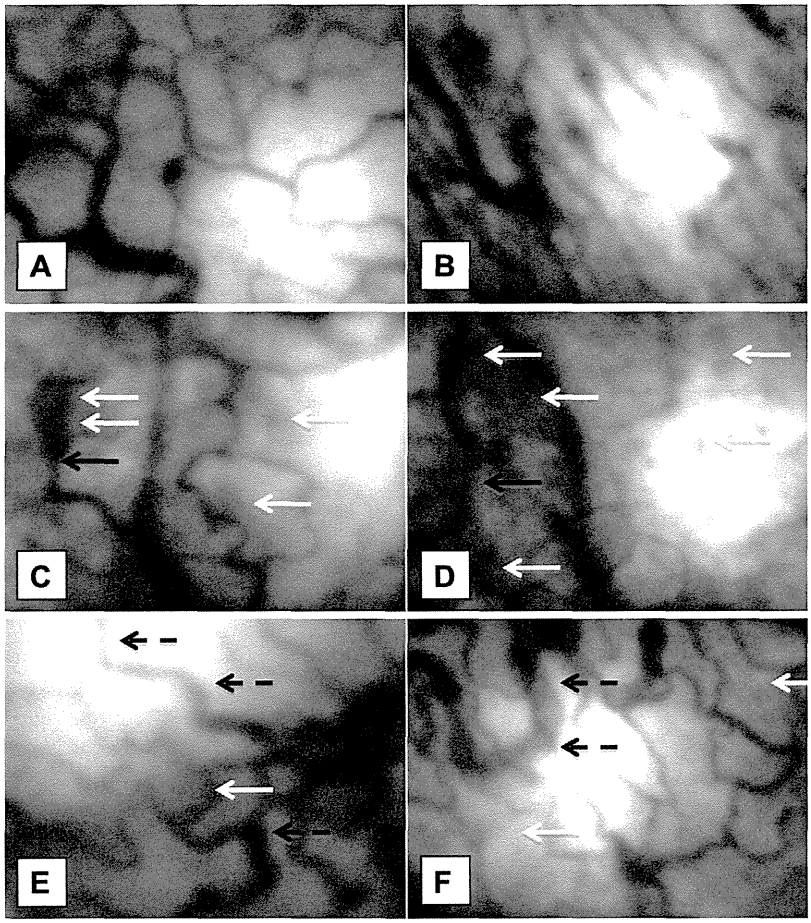

Figure 1. Images of submucosal capillaries of the bladder obtained using pencil lens charge-coupled device microscopy system. Magnification approximately ×400, and horizontal and vertical image size 400 and 300 μm, respectively. **(A-F)** Typical images of submucosal capillary at bladder base and dome shown for all 3 groups. Images from control group **(C,D)** show chronic ischemic capillary dysfunction with sporadic microvascular hemorrhage (white arrow), scattered microvascular thrombosis (no blood flow; black arrows), and irregular capillary flow (sludgy erythrocyte columns; white arrow). Images from tamsulosin group **(E,F)** show improvement in SCB, with sporadic microvascular hemorrhage (white arrow), scattered microvascular thrombosis (black arrows), and irregular capillary flow (sludgy erythrocyte columns; thick white arrow), with SCB wider (black dot arrows) than SCB of BOO rats (control group).

the bladder. LDBF has a disadvantage, in that the flow is measured using a single point-type probe in a given region (hemisphere, radius 1 mm), and the vessel density in the measured region has a substantial effect on the results, rendering this method inefficient.[10-12] Furthermore, the layer of the bladder wall (ie, muscular or mucosal) or the type of target vessel (ie, artery, vein, or capillary) that is measured cannot be identified. We have previously reported the assessment of the microheterogeneity of blood flow from the base to the dome and from the mucosal to the muscle layers in the urinary bladder of rats using high-resolution digital radiography. Using this technique, it was revealed that the blood flow of the mucosal layer, including the SCB, increased more at the base than at the dome.[13] Azadzoi et al[12] found marked regional differences in the bladder blood flow in rabbits, and LDBF was used to show that the base of the bladder received much greater flow than the dome. Matsumoto et al[14] assessed the changes in rabbit bladder vasculature associated with bladder filling and changes in the thickness of the bladder wall. They reported that the bladder veins were compressed and squeezed together when the bladder was 25% full but that the bladder arteries and arterioles remained open. This phenomenon was confirmed by the decrease in bladder blood flow observed with LDBF during the early phase of bladder filling. The PLCMS has a significant advantage because it can measure the flow velocity of the red blood cells in a specific blood vessel; a submucosal capillary can be continuously tracked over time when the bladder is full or empty, and the velocity of the blood flow in the same capillary vessel can be measured.[8]

In the present study, direct measurement of the blood flow in the SCB using the PLCMS confirmed ischemic injury to the submucosal blood flow caused by chronic outlet obstruction. The causes of chronic ischemia of the

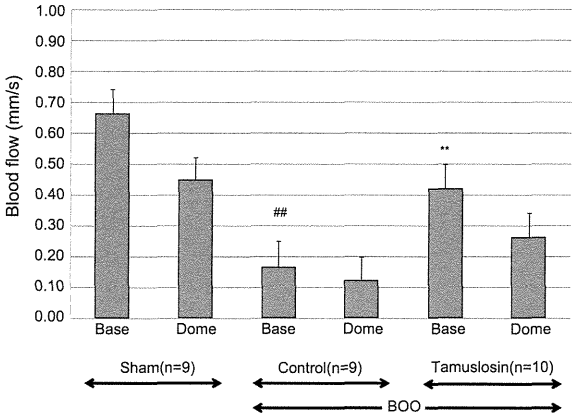

Figure 2. Effect of tamsulosin on blood flow through submucosal capillaries at bladder base and dome of bladder outlet obstruction rats. Blood flow in submucosal capillaries of the bladder measured using pencil lens charge-coupled device microscopy system (n = 9 for sham-operated group, n = 9 for control group, and n = 10 for tamsulosin group). $^{\#}P < .05$, $^{\#\#}P < .01$ vs sham group (Student's *t* test); $*P < .05$, $**P < .01$ vs control group (Dunnett's multiple comparison test).

bladder in the clinical setting are thought to be multifactorial, including the bladder overdistension caused by lower urinary tract obstruction.[4] In a rabbit model of chronic bladder ischemia caused by injury to the vascular endothelial cells of the iliac artery, moderate bladder ischemia (40%-60%) enhanced detrusor overactivity and the carbachol-induced contractile response of the smooth muscles of the bladder, suggesting that bladder ischemia could be 1 of the causes of an overactive bladder.[12] Decreased bladder blood flow has been reported in rat,[15,16] rabbit,[17,18] and pig[19] models of partial urethral obstruction. Furthermore, persistent decreased blood flow has been reported in patients with BPH and patients with detrusor overactivity, even after transurethral resection of the prostate.[20] These findings suggest that the decreased bladder blood flow associated with urethral obstruction might be involved in producing the storage symptoms experienced by patients with BPH.

In the present study, we assessed the effect of tamsulosin administration on the impaired blood flow caused by BOO at the base and dome of the bladder. We found that compared with the control rats, which were administered saline, the BOO rats administered tamsulosin showed significant increases in the blood flow velocity through the submucosal capillaries. Das et al[16] reported that doxazosin increased the bladder blood flow in rats with BOO. Okutsu et al[21] evaluated messenger ribonucleic acid expression of ARs in rat bladder arteries and found that α_{1A} and α_{1D} were the most common AR subtypes, and that the α_{1B} adrenoceptor subtype was almost absent. In addition, they assessed the blood flow in the bladder using the fluoromicrosphere method and reported that tamsulosin at the same dose used in our study increased bladder blood flow in BOO model rats.[21] From the present data and previously reported findings, we hypothesized that tamsulosin could have a beneficial effect in improving storage symptoms in patients with BPH by improving bladder ischemia caused by BOO, by way of either or both α_{1A}- and α_{1D}-ARs.

Our study had some limitations, especially when extrapolating our results to human patients. The effective dose in the present study was preliminarily confirmed to be comparable to the clinically effective dose from the perspective of the plasma concentration area under the plasma concentration curve for the unbound compound.[21] However, it is difficult to compare the physiological significance of the increase in intravesical pressure between the present experimental model rats and patients with BPH. Thus, the effectiveness of tamsulosin needs to be confirmed in human patients with BPH.

CONCLUSION

The PLCMS was used to visualize the bladder microcirculation in BOO rats and quantitatively assess the blood flow in the SCB by measuring its velocity. The findings from the present study suggest that chronic ischemia of the bladder wall might be a cause of detrusor overactivity in lower urinary tract obstruction. Tamsulosin improved the impaired blood flow caused by BOO; this could be 1 of the mechanisms by which tamsulosin improves the storage symptoms in patients with BPH.

References

1. Peters TJ, Donovan JL, Kay HE, et al. The International Continence Society "Benign Prostatic Hyperplasia" Study: the bothersomeness of urinary symptoms. *J Urol.* 1997;157:885-889.
2. Yokoyama O, Yusup A, Oyama N, et al. Improvement in bladder storage function by tamsulosin depends on suppression of C-fiber urethral afferent activity in rats. *J Urol.* 2007;177:771-775.
3. Pinggera GM, Mitterberger M, Pallwein L, et al. Alpha-blockers improve chronic ischaemia of the lower urinary tract in patients with lower urinary tract symptoms. *BJU Int.* 2008;101:319-324.
4. Matsumoto S, Uemura H. Examination of the mechanism of ameliorating effect of alpha 1-blocker on storage symptoms associated with benign prostatic hyperplasia. *Hinyokika Kiyo.* 2008;54:453-456 [in Japanese].
5. Tanaka T, Noiri E, Yamamoto T, et al. Urine human L-FABP is a potential biomarker to predict COX-inhibitor induced renal injury. *Nephron Exp Nephrol.* 2008;108:e19-e26.
6. Yamamoto T, Tada T, Brodsky SV, et al. Intravital videomicroscopy of peritubular capillaries in renal ischemia. *Am J Physiol Renal Physiol.* 2002;282:F1150-F1155.
7. Yamamoto T, Hayashi K, Tomura Y, et al. Direct in vivo visualization of renal micro-circulation by intravital CCD videomicroscopy. *Exp Nephrol.* 2001;9:150-155.
8. Mizuno H, Yamamoto T, Okutsu H, et al. Effect of tamsulosin on bladder microcirculation in a rat ischemia-reperfusion model, evaluated by pencil lens charge-coupled device microscopy system. *Urology.* 2010;76:1266.e1-1266.e5.
9. Ohtake A, Ukai M, Saitoh C, et al. Effect of tamsulosin on spontaneous bladder contraction in conscious rats with bladder outlet obstruction: comparison with effect on intraurethral pressure. *Eur J Pharmacol.* 2006;545:185-191.

10. Siroky MB, Krane RJ, Pontari M, et al. Effect of bladder filling and contraction on bladder micro-circulation. *Neurourol Urodyn.* 1993;12:400-401.
11. Bajory Z, Hutter J, Krombach F, et al. Microcirculation of the urinary bladder in a rat model of ischemia-reperfusion-induced cystitis. *Urology.* 2002;60:1136-1140.
12. Azadzoi KM, Tarcan T, Kozlowski R, et al. Overactivity and structural changes in the chronically ischemic bladder. *J Urol.* 1999;162:1768-1778.
13. Kimura T, Yamamoto T, Sone A, et al. Assessment of micro-heterogeneity of blood flow in the rat urinary bladder by high-resolution digital radiography. *BJU Int.* 2005;95:895-897.
14. Matsumoto S, Chichester P, Kogan BA, et al. Structural and vascular response of normal and obstructed rabbit whole bladders to distension. *Urology.* 2003;62:1129-1133.
15. Saito M, Yokoi K, Ohmura M, et al. Effects of partial outflow obstruction on bladder contractility and blood flow to the detrusor: comparison between mild and severe obstruction. *Urol Int.* 1997;59: 226-230.
16. Das AK, Leggett RE, Whitbeck C, et al. Effect of doxazosin on rat urinary bladder function after partial outlet obstruction. *Neurourol Urodyn.* 2002;21:160-166.
17. Schröder A, Chichester P, Kogan BA, et al. Effect of chronic bladder outlet obstruction on blood flow of the rabbit bladder. *J Urol.* 2001;165:640-646.
18. Lin AT-L, Chen M-T, Yang C-H, et al. Blood flow of the urinary bladder: effects of outlet obstruction and correlation with bioenergetic metabolism. *Neurourol Urodyn.* 1995;14:285-292.
19. Greenland JE, Hvistendahl JJ, Andersen H, et al. The effect of bladder outlet obstruction on tissue oxygen tension and blood flow in the pig bladder. *BJU Int.* 2000;85:1109-1114.
20. Mitterberger M, Pallwein L, Gradl J, et al. Persistent detrusor overactivity after transurethral resection of the prostate is associated with reduced perfusion of the urinary bladder. *BJU Int.* 2007;99: 831-835.
21. Okutsu H, Matsumoto M, Hanai T, et al. Effects of tamsulosin on bladder blood flow and bladder function in rats with bladder outlet obstruction. *Urology.* 2010;75:235-240.

BASIC RESEARCH www.jasn.org

Serum-Starved Adipose-Derived Stromal Cells Ameliorate Crescentic GN by Promoting Immunoregulatory Macrophages

Kazuhiro Furuhashi,* Naotake Tsuboi,* Asuka Shimizu,* Takayuki Katsuno,* Hangsoo Kim,* Yosuke Saka,* Takenori Ozaki,* Yoshikazu Sado,† Enyu Imai,* Seiichi Matsuo,* and Shoichi Maruyama*

*Department of Nephrology, Internal Medicine, Nagoya University Graduate School of Medicine, Showa-ku, Nagoya, Aichi, Japan; and †Division of Immunology, Shigei Medical Research Institute, Okayama, Japan

ABSTRACT

Mesenchymal stromal cells (MSCs) derived from adipose tissue have immunomodulatory effects, suggesting that they may have therapeutic potential for crescentic GN. Here, we systemically administered adipose-derived stromal cells (ASCs) in a rat model of anti-glomerular basement membrane (anti-GBM) disease and found that this treatment protected against renal injury and decreased proteinuria, crescent formation, and infiltration by glomerular leukocytes, including neutrophils, $CD8^+$ T cells, and $CD68^+$ macrophages. Interestingly, ASCs cultured under low-serum conditions (LASCs), but not bone marrow-derived MSCs (BM-MSCs), increased the number of immunoregulatory $CD163^+$ macrophages in diseased glomeruli. Macrophages cocultured with ASCs, but not with BM-MSCs, adopted an immunoregulatory phenotype. Notably, LASCs polarized macrophages into $CD163^+$ immunoregulatory cells associated with IL-10 production more efficiently than ASCs cultured under high-serum conditions. Pharmaceutical ablation of PGE_2 production, blocking the EP_4 receptor, or neutralizing IL-6 in the coculture medium all significantly reversed this LASC-induced conversion of macrophages. Furthermore, pretreating LASCs with aspirin or cyclooxygenase-2 inhibitors impaired the ability of LASCs to ameliorate nephritogenic IgG-mediated renal injury. Taken together, these results suggest that LASCs exert renoprotective effects in anti-GBM GN by promoting the phenotypic conversion of macrophages to immunoregulatory cells, suggesting that LASC transfer may represent a therapeutic strategy for crescentic GN.

J Am Soc Nephrol 24: ●●●–●●●, 2013. doi: 10.1681/ASN.2012030264

Mesenchymal stromal cells (MSCs; formally known as mesenchymal stem cells) derived from cord blood, bone marrow, connective, and adipose tissues have the capacity to differentiate into multiple mesenchymal lineages, including osteoblasts, chondrocytes, and adipocytes.[1,2] Apart from the classic regenerative property of MSCs, mounting evidence from studies focusing on bone marrow–derived MSCs (BM-MSCs) suggests that MSCs can modulate inflammatory immune responses.[3–8] This effect is currently believed to be mediated through MSC-derived growth factors, cytokines, and PGs, which negatively regulate inflammatory immune responses and the proliferation of leukocytes and resident cells that are systemically or locally activated.[9–14]

As a potential clinical therapeutic agent, ASCs may have a number of practical advantages over BM-MSCs relating to their abundance and availability.[15,16] Several studies have demonstrated ASC-mediated immunomodulation of particular leukocyte subsets, including lymphocytes and dendritic cells.[14,17,18] This immunomodulatory property of ASCs has already been exploited for therapeutic intervention in inflammatory diseases. A number of clinical trials are

Received March 13, 2012. Accepted December 20, 2012.

Published online ahead of print. Publication date available at www.jasn.org.

Correspondence: Dr. Naotake Tsuboi, Department of Nephrology, Internal Medicine, Nagoya University Graduate School of Medicine, 65 Tsurumai-cho, Showa-ku, Nagoya 466-8550, Japan. Email: tsubotake05@med.nagoya-u.ac.jp

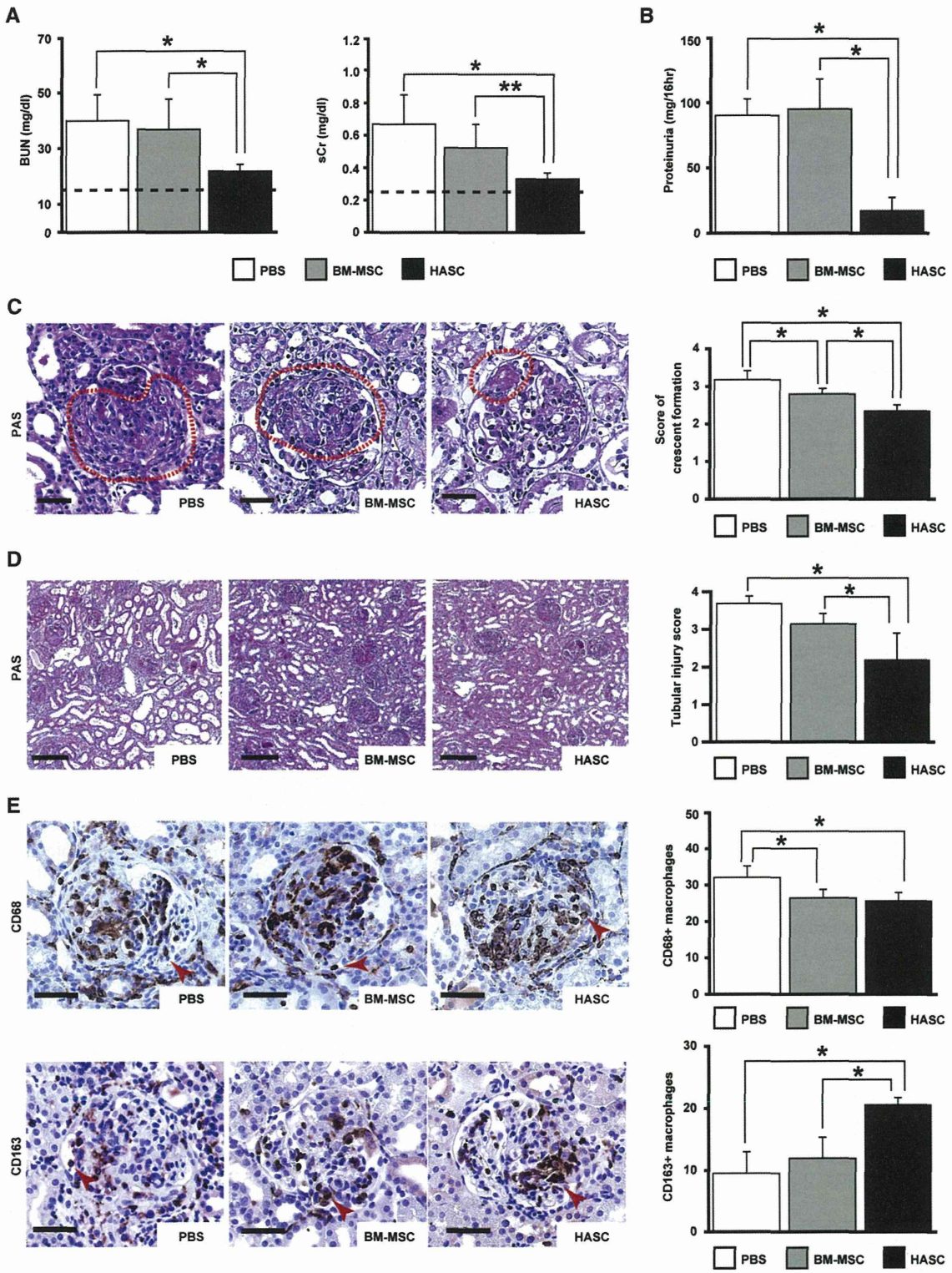

Figure 1. Systemic administration of BM-MSCs and HASCs has a protective effect against rat anti-GBM GN. (A) Analysis of renal function in BM-MSC–treated and HASC-treated rats after induction of anti-GBM GN. The levels of both BUN (left) and sCr (right) at day 7 after TF78 injection are significantly reduced in the HASC-treated group (n=7) compared with the PBS-treated (n=7) and BM-MSC–treated (n=13) groups. Dotted line indicates the value in healthy rats (n=3). (B) 16-hour proteinuria value on day 5 in the HASC-treated group

underway in which ASCs have been administered to patients with autoimmune disorders, including graft versus host disease, Crohn's disease, multiple sclerosis, and SLE.[19–21] However, the precise mechanism of ASC-mediated immunomodulation is unclear, and a direct comparison of the efficacy of ASCs versus that of BM-MSCs has not been undertaken.

For cell transfer therapy, a reduction in the concentration of serum in MSC cultures is beneficial for recipients because this reduces concerns about infection with microorganisms or pathogenic proteins originating from culture media. However, the concentration of serum in culture media influences MSC expansion *ex vivo*, and thus affects cell proliferation. Moreover, the serum concentration modulates regeneration and immunomodulation.[14,15] For instance, the proliferation rate of rat BM-MSCs in low-serum media is significantly lower than in high-serum media.[14,15] In contrast, human ASCs grown under low-serum conditions (LASCs) display comparable growth to human BM-MSCs cultured in high-serum media.[14,15] Of further interest, human LASCs more effectively suppress phytohemagglutinin-stimulated T cell proliferation *in vitro* than ASCs grown under high-serum conditions (HASCs), despite a similar ability of the two cell types to differentiate into the mesenchymal cell lineage.[14] Therefore, LASC-mediated immunomodulation may have great potential as a cell-based therapy.

Anti-GBM GN is characterized by poor prognostic GN with crescent formation (crescentic GN [CGN]), which rapidly results in renal failure after onset of the disease.[22] This is characteristic of Goodpasture's disease in humans, in which patients may also occasionally present with pulmonary hemorrhage, with dire consequences. Although effector responses by neutrophils, macrophages/monocytes, T lymphocytes, and immune regulation by regulatory T cells and alternatively activated macrophages have been extensively investigated as part of efforts to understand the distinct mechanisms that cause glomerular crescent formation,[23–29] a potent and feasible therapeutic strategy to inhibit leukocyte effector functions and/or augment their regulatory functions has not emerged for CGN patients. Thus, in this study, we investigated the potential of ASCs to exert immunomodulatory functions in anti-GBM GN.

RESULTS

Administration of ASCs Ameliorates Disease Activity in a Rat Anti-GBM GN Model

The anti-inflammatory properties of ASCs were compared with those of BM-MSCs in a rat anti-GBM GN model. We administered 2.0×10^6 BM-MSCs or ASCs cultured under high-serum conditions (20% FBS) (HASCs) to TF78-treated WKY/NCrj rats for 6 consecutive days. Elevations in BUN, serum creatinine (sCr), and proteinuria in BM-MSC–treated rats were comparable with those in untreated rats. In contrast, HASC treatment significantly attenuated renal dysfunction and proteinuria compared with the BM-MSC–treated and control groups (Figure 1, A and B). Renal histologic analysis on day 7 revealed milder glomerular crescent formation and tubular damage in HASC-treated animals than in BM-MSC–treated rats (Figure 1, C and D). Moreover, a marked increase in the $CD163^+$ macrophage population, which represents alternatively activated M2 macrophages,[30,31] was observed in HASC-treated rats versus the BM-MSC–treated group (Figure 1E). Because the number of infiltrated $CD68^+$ cells in the glomerulus (which represent infiltrated macrophages or dendritic cells) was similar between the BM-MSC–treated and HASC-treated groups (Figure 1E), we hypothesized that ASCs may exert their function by phenotypic conversion of macrophages into immunoregulatory cells in inflamed glomeruli after anti-GBM GN induction.

Low-Serum Culture Conditions Amplify the Renoprotective Effects of ASCs

Our previous reports demonstrated the therapeutic superiority of LASC transfer versus HASC transfer in several animal models.[14,15,32] Systemic or local administration of LASCs improved rat ischemic hind limb injury[15] and folic acid–induced acute renal tubular injury,[32] and impeded production of antibodies against exogenous porcine red blood cells.[14] Moreover, LASCs produce higher amounts of hepatocyte growth factor (HGF) and vascular endothelial growth factor (VEGF) *in vitro* than HASCs (Supplemental Figure 1C). Therefore, we examined whether LASCs exhibit enhanced renoprotective effects compared with HASCs in anti-GBM GN. Administration of LASCs to TF78-treated rats significantly improved survival over the 28-day observation period (Figure 2A). Functional analysis of the diseased kidneys also demonstrated a dramatic reduction in BUN, sCr, and proteinuria in LASC-treated versus HASC-treated rats (Figure 2B). Despite comparable TF78 deposition on the GBM in both HASC- and LASC-treated groups (Supplemental Figure 2), histologic analysis clearly demonstrated that glomerular crescent formation was significantly reduced on days 4, 7, and 14 in LASC-treated rats compared with the HASC-treated group (43% decrease in glomerular crescent formation in HASC-treated rats versus a 75% decrease in LASC-treated rats compared with the control

(n=7) compared with the PBS-treated (n=7) and BM-MSC–treated (n=6) groups. (C and D) Representative micrographs of PAS-stained renal sections harvested on day 7. Histologic scores for glomerular crescent formation (C) and tubular injury (D) in the indicated groups (n=6–7 per group) at day 7 are determined semiquantitatively. Dotted areas indicate glomerular crescent formation. (E) Representative micrographs of glomeruli stained with specific monoclonal IgGs for rat CD68 (upper) and CD163 (lower) on day 7 after disease induction. Accumulation of $CD68^+$ and $CD163^+$ (arrowheads) macrophages per glomerulus at day 7 is also determined. All data are mean ± SD. *P<0.01 and **P<0.05 as determined by ANOVA. Scale bars indicate 50 μm, except for the micrograph illustrating tubular injury, in which the bar indicates 200 μm. PAS, periodic acid–Schiff.

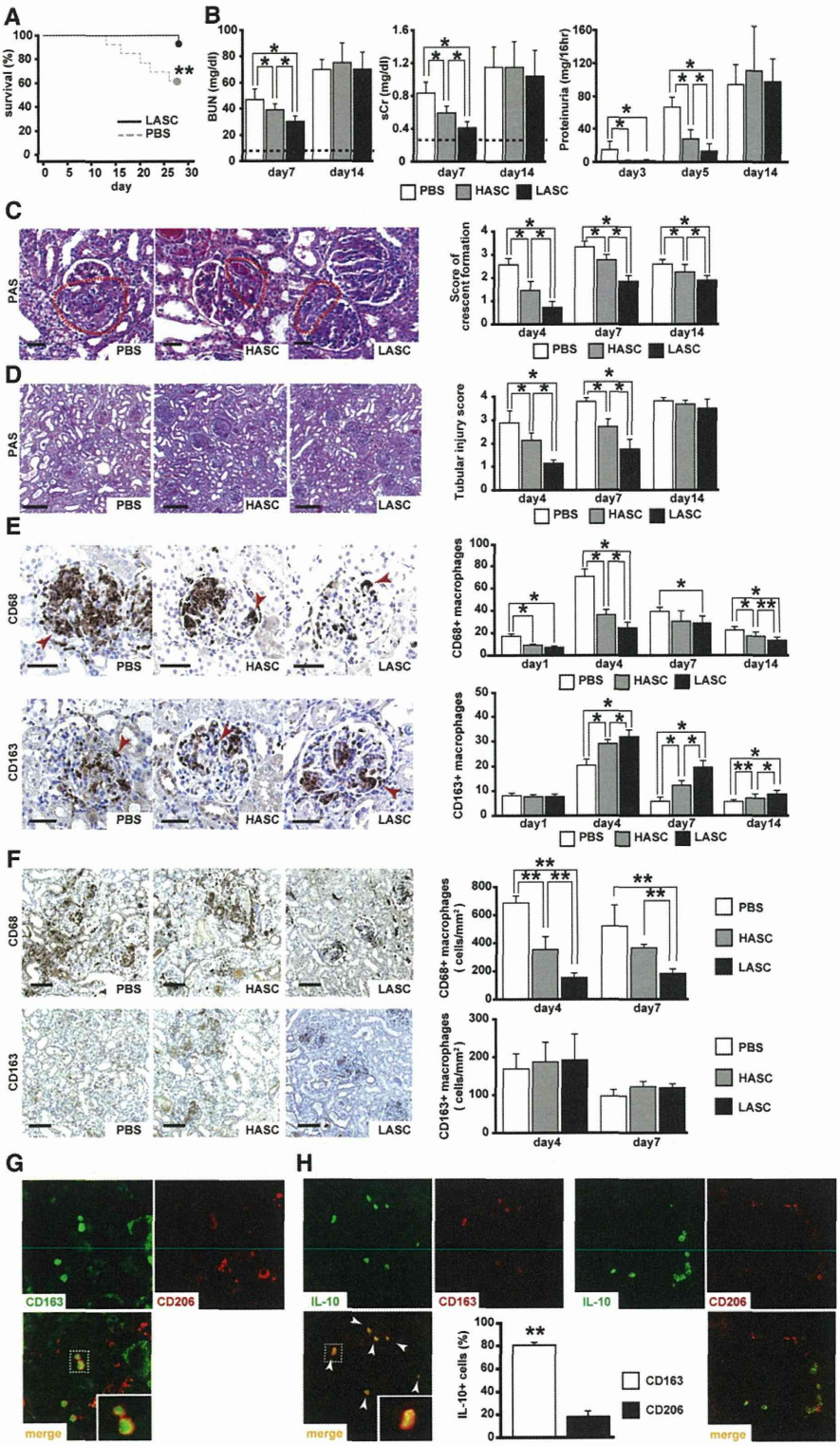

Figure 2. Comparison of HASC and LASC administration for ASC-mediated protection against anti-GBM GN. (A) Survival curves for LASC-treated (n=14) and untreated (n=13) rats after anti-GBM antibody injection. (B) Renal function is assessed by determining BUN and sCr concentrations in PBS-treated (n=7), HASC-treated (n=7), and LASC-treated (n=8) anti-GBM GN rats on days 7 and 14. Dotted lines indicate value in healthy rats (n=3). The concentration of protein in the urine of rats in each group measured on days 3, 5, and 14

group on day 4; Figure 2C). The decrease in the number of $CD68^+$ glomerular macrophages was more significant in LASC-treated rats, and a significant increase in the number of glomerular $CD163^+$ macrophages was observed in LASC-treated rats over the entire study period compared with the HASC-treated and control groups (Figure 2E).

In addition to amelioration of glomerular damage, renal tubular injury was also attenuated by LASC treatment at days 4 and 7 (Figure 2D). Notably, there was no significant difference in the accumulation of $CD163^+$ macrophages in the renal interstitium between the experimental groups, despite the reduced number of $CD68^+$ cells in the LASC-treated group (Figure 2F). Moreover, circulating monocytes isolated from LASC-treated rats with anti-GBM GN did not exhibit an increase in cytosolic or surface levels of CD163 compared with circulating monocytes isolated from diseased rats treated with PBS (Supplemental Figure 3). Together, these data indicate that ASCs promote an increase in the number of $CD163^+$ cells specifically and locally at inflamed glomeruli.

Immunohistochemical analysis of diseased glomeruli revealed that the expression of CD206, another specific marker for alternatively activated M2 macrophages,[31,33] did not specifically overlap with that of CD163 (Figure 2G). This is suggestive of heterogeneous differentiation of macrophages into M2 cells in diseased glomeruli.[30] We then investigated whether $CD163^+$ or $CD206^+$ cells produce IL-10, a representative anti-inflammatory cytokine induced by LASC treatment, and confirmed that expression of IL-10 is higher in $CD163^+$ cells than in $CD206^+$ cells in diseased glomeruli (Figure 2H).

It has been proposed that glomerular inflammation in anti-GBM GN is a multistep process that includes glomerular recruitment of leukocytes such as neutrophils, monocytes/macrophages, and lymphocytes, as well as production of proteinases, cytokines/chemokines, and oxygen radicals by inflammatory cells.[23–26,34,35] Histologic assessment of neutrophils and T cells in diseased glomeruli after TF78 injection revealed a decrease in the accumulation of neutrophils and $CD8^+$ T cells, but not $CD4^+$ T cells, in both HASC- and LASC-treated rats; however, these differences were limited to day 1 (Supplemental Figure 4). Together, these results indicate that during the initial phase, LASCs prevent recruitment of broad leukocyte subsets, including $CD8^+$ T cells, neutrophils, and $CD68^+$ macrophages, and then play an anti-inflammatory role in subsequent phases by promoting an increase in the number of $CD163^+$ macrophages in glomeruli.

Profiles of IL-1β, IL-12 p70, and IL-10 Cytokines in the Renal Cortex of Diseased Kidneys of Rats Treated with ASCs

One subtype of alternatively activated M2 macrophages is known to play an immunoregulatory role by generating IL-10, an immunosuppressive cytokine. To clarify whether ASC-mediated attenuation of rat anti-GBM GN results from a phenotypic switch of renal macrophages to $CD163^+$ cells, we examined cytokine profiles in the renal cortex of diseased animals. Renal concentrations of IL-1β and IL-12 p70, representative proinflammatory cytokines, were significantly decreased in LASC-treated animals at day 4 after disease induction, but no differences in the concentrations of these cytokines were observed on day 7 compared with the HASC- and PBS-treated groups. In contrast, higher IL-10 levels were observed in the LASC-treated group than in both the HASC-treated and control groups on both days 4 and 7 (Figure 3A). Notably, solid correlations existed between the IL-10 concentration and the number of glomerular $CD163^+$ infiltrating cells and sCr concentration in all experimental groups (Figure 3, B and C). These results strongly suggest that administration of ASCs, in particular LASCs, protects against TF78-mediated renal damage by converting macrophages from an inflammatory to an immunoregulatory phenotype.

Recruitment of HASCs and LASCs into Diseased Kidneys Is Comparable

It is important to demonstrate the accumulation of circulating exogenous ASCs in inflamed organs where their therapeutic potential is observed. Therefore, we examined the delivery of carboxyfluorescein succinimidyl ester (CFSE)–treated ASCs into diseased rat kidneys. Intravenous administration of ASCs *via* the tail vein led to their entrapment in the liver and lung at day 5, because these are the first organs encountered and possess large vascular beds. After day 5, the cells were distributed in multiple organs (Figure 4A and Supplemental

(n=7 per group). (C and D) Representative micrographs of kidney sections stained with PAS on day 4 to assess crescent formation (C) and on day 7 to assess tubular injury (D). Histologic scores for glomerular crescent formation and tubular injury are determined on days 4, 7, and 14 in the indicated groups (n=6–8 per group). Dotted areas indicate glomerular crescent formation. (E and F) Representative micrographs of glomeruli at day 4 and the interstitium at day 7, stained with specific antibodies against $CD68^+$ and $CD163^+$ macrophages. Glomerular (E) and interstitial (F) accumulation of $CD68^+$ and $CD163^+$ cells at indicated time points (n=7–8 per group). All data are mean ± SD. *P<0.01 and **P<0.05 as determined by ANOVA. (G) Representative micrographs of glomeruli obtained by double immunostaining for CD163 (green) and CD206 (red) at day 4 after disease induction with LASC treatment. The inset shows $CD163^+CD206^+$ macrophages under high-power magnification. (H) Representative micrographs illustrating double immunostaining for IL-10 (green) and CD163 (red) or CD206 (red) and quantification of $CD163^+$ or $CD206^+$ cells expressing IL-10 at day 4 after disease induction with LASC treatment. Arrowheads indicate $IL10^+CD163^+$ cells in the glomerulus and the inset shows $IL\text{-}10^+CD163^+$ cells under high-power magnification (n=4 per group). All data are mean ± SD. **P<0.05 as determined by t test. Scale bars, 50 μm in C and E; 100 μm in F; 200 μm in D. PAS, periodic acid–Schiff.

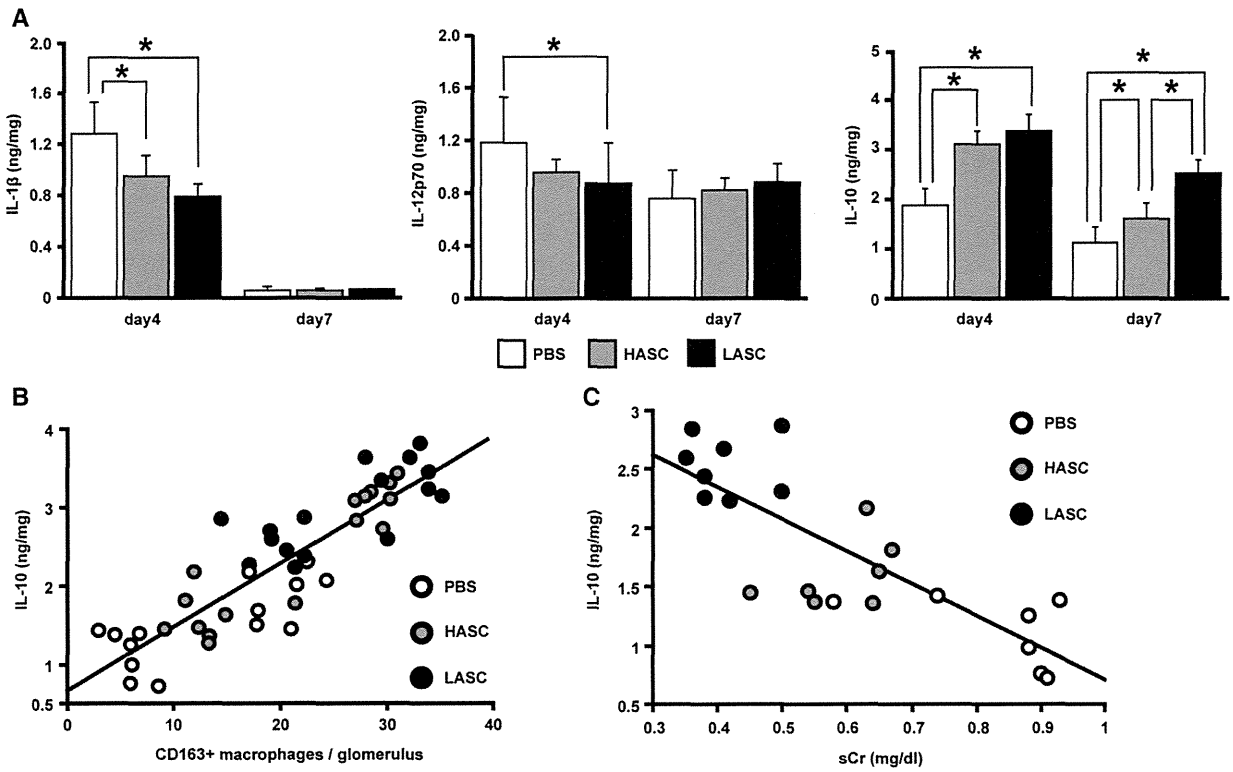

Figure 3. Renal cytokine profiles in ASC-treated anti-GBM GN rats. (A) Concentrations of the proinflammatory cytokines IL-1β and IL-12p70 and the anti-inflammatory cytokine IL-10 in the kidneys of PBS-treated, HASC-treated, and LASC-treated anti-GBM GN rats. Cytokine concentrations in nanograms per milligram of total protein in homogenates from renal cortex are determined. All data are mean ± SD. *$P<0.01$ as determined by ANOVA (n=7–8 per group). (B and C) Linear regression analysis reveals a tight correlation between renal IL-10 concentration and glomerular accumulation of CD163$^+$ macrophages at days 4 and 7 (B) (r^2=0.77) and sCr (C) (r^2=0.66) at day 7. Each dot represents an individual kidney sample from a PBS-treated, HASC-treated, and LASC-treated rat.

Figure 5). CFSE$^+$ cells were observed primarily in the glomeruli but were also present in glomerular crescents and peritubular capillaries on day 5 (Figure 4A); however, they were not evident from day 14 onward (Figure 4B). Importantly, no difference between HASC- and LASC-treated rats with respect to the number of glomerular CFSE$^+$ cells was observed at day 5 (Figure 4C), suggesting that differential accumulation of HASCs and LASCs in the kidney cannot explain the differential renoprotective effects of these two cell populations.

LASCs Directly Promote Functional Polarization of Macrophages into Immunoregulatory M2 Cells

We conducted *in vitro* studies to explore the possibility that LASCs can directly polarize macrophages into an immunoregulatory phenotype. In a coculture system involving MSCs and rat peritoneal macrophages, LASCs strongly induced IL-10 production and enhanced the number of CD163$^+$ macrophages compared with BM-MSCs and HASCs (Figure 5, A and B). LASC-mediated induction of CD163 expression on macrophages was also evident by real-time imaging (Supplemental Figure 6). However, the number of CD68$^+$ macrophages significantly decreased when cocultured with LASCs (Figure 5B). LASCs also induced expression of CD206, another marker of alternatively activated M2 macrophages,[31,33] but the proportion of CD206^{high+}CD163$^+$ cells was small (around 6%) in the macrophage population cocultured with LASCs (Figure 5, E and F).

Next, we cultured peritoneal macrophages with LASCs in a trans-well plate system that prevents close contact between the LASCs and macrophages in order to determine whether cell-to-cell contact is needed for polarization of macrophages to CD163$^+$ cells. Induction of CD163 expression on macrophages was observed in this culture system, indicating that LASC-derived soluble factors play a role in macrophage M2 polarization. However, a further increase in the number of CD163$^+$ macrophages was observed in the absence of the membrane insert, suggesting that cell contact enhances this process (Figure 5C). Although LASCs injected *in vivo* successfully accumulated in the glomeruli, the number of cells was relatively small. To evaluate the efficiency with which LASCs induce a phenotypic change in macrophages, we incubated peritoneal macrophages with LASCs at ratios ranging from

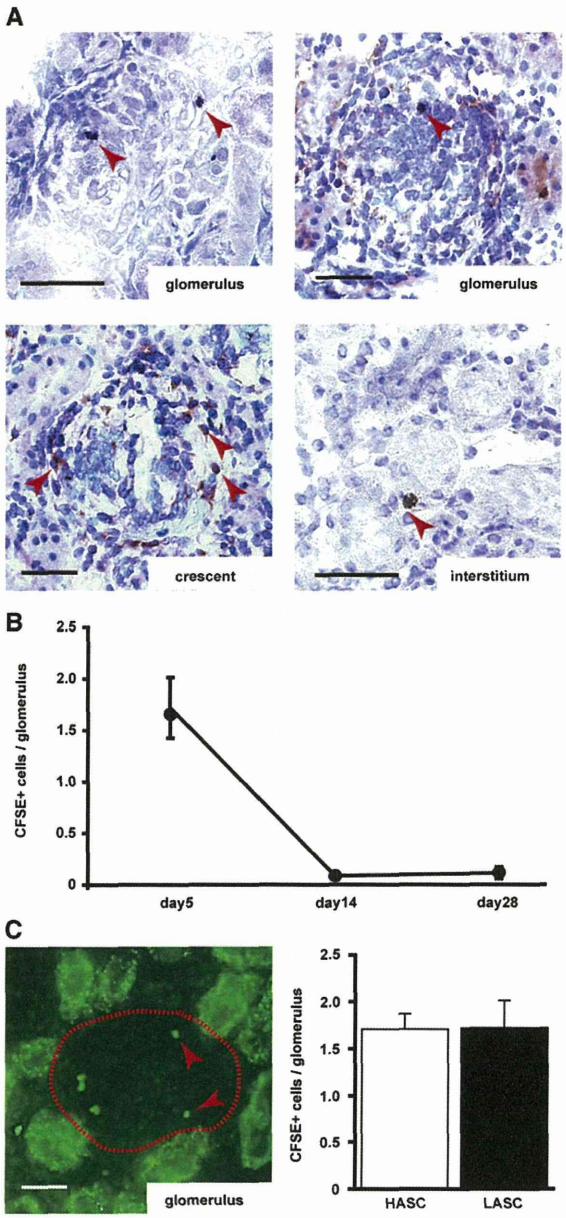

Figure 4. Recruitment of transferred ASCs in the kidneys of anti-GBM GN rats. (A) CFSE-stained LASCs are administered to anti-GBM GN rats on days 0–4 *via* the tail vein, and the kidneys are harvested on day 5. Exogenous LASCs (arrowheads) in frozen sections are identified using a polyclonal anti-CFSE antibody. In kidneys, $CFSE^+$ cells are observed in the glomeruli, glomerular crescents, and interstitium. (B) Glomerular accumulation of $CFSE^+$ cells at days 5, 14, and 28 is shown. (C) A representative immunofluorescence image of kidney tissue from an LASC-treated anti-GBM GN rat on day 5 (left). Dotted area indicates a glomerulus. Glomerular accumulation of $CFSE^+$ cells (arrowheads) from HASC- or LASC-treated rats is analyzed (right). No significant difference is observed between HASC-treated and LASC-treated rats with respect to the number of glomerular $CFSE^+$ ASCs. Data are mean ± SD (n=4 per group). Scale bar, 50 μm.

1:1 to 1000:1. Remarkably, an individual LASC could induce a phenotypic change on 200 macrophages (Figure 5D). Together, these data provide compelling evidence that a very small number of LASCs may be sufficient to promote polarization of macrophages into M2 cells in the inflamed glomerulus.

PGE2 Produced by LASCs Strongly Induces the Phenotypic Conversion of Macrophages into Immunoregulatory Cells

A variety of cytokines, growth factors, and PGs that pleiotropically affect tissue regeneration, cell proliferation, and immune modulation are produced by MSCs. In particular, PGE2 derived from BM-MSCs was recently described as playing a critical role in stimulating IL-10 production by macrophages.[12] Therefore, we hypothesized that ASC-derived PGE2 may be a key modulator of macrophage conversion to an immunoregulatory phenotype in our anti-GBM GN experimental model. Despite comparable amounts of 15d-PGJ2, a metabolite of PGD2, in the supernatants of MSCs cultured with and without macrophages, LASCs cultured in the absence of macrophages constitutively secreted abundant amounts of PGE2 compared with BM-MSCs and HASCs (Figure 6A). Secretion of PGE2 by LASCs was even more prominent in cocultures with macrophages (Figure 6B). Moreover, pharmaceutical ablation of LASC-derived PGE2 synthesis by a cyclooxygenase-2 (COX-2) inhibitor or aspirin and blocking of the EP4 receptor (but not the PGD receptor) clearly impaired macrophage conversion to $CD163^+$ cells in the coculture system (Figure 6, C–E). *In vivo* pharmaceutical ablation of LASC-derived PGE2 synthesis by a COX-2 inhibitor or aspirin also decreased the therapeutic potency of LASCs and the induction of glomerular macrophage polarization to $CD163^+$ cells (Figure 7). Treatment with synthetic PGE2 alone resulted in a significant increase in the conversion of cultured macrophages into $CD163^+$ cells (Figure 6F), but was less efficient than LASC treatment, suggesting that interaction between LASCs and macrophages as well as persistent stimulation or other humoral factors are also required.

LASC-Derived IL-6 Promotes Conversion of Macrophages to the Immunoregulatory Phenotype

As discussed above, LASC-derived PGE2 alone was not sufficient to cause conversion of macrophages to an immunoregulatory phenotype. Whereas reports indicate that IL-10, M-CSF, IL-4, and IL-13 promote differentiation of macrophages into M2 cells,[31,36] these cytokines were largely absent in LASC supernatants in our study (data not shown). However, secretion of considerable amounts of IL-6 by LASCs was observed (Figure 8A). Interestingly, polarization of macrophages to $CD163^+$ cells was significantly reversed by antibody neutralization of IL-6 in the culture supernatant, and was induced by IL-6 stimulation *in vitro* (Figure 8, B and C). These data suggest that besides PGE2, LASC-derived IL-6 may also mediate macrophage polarization.

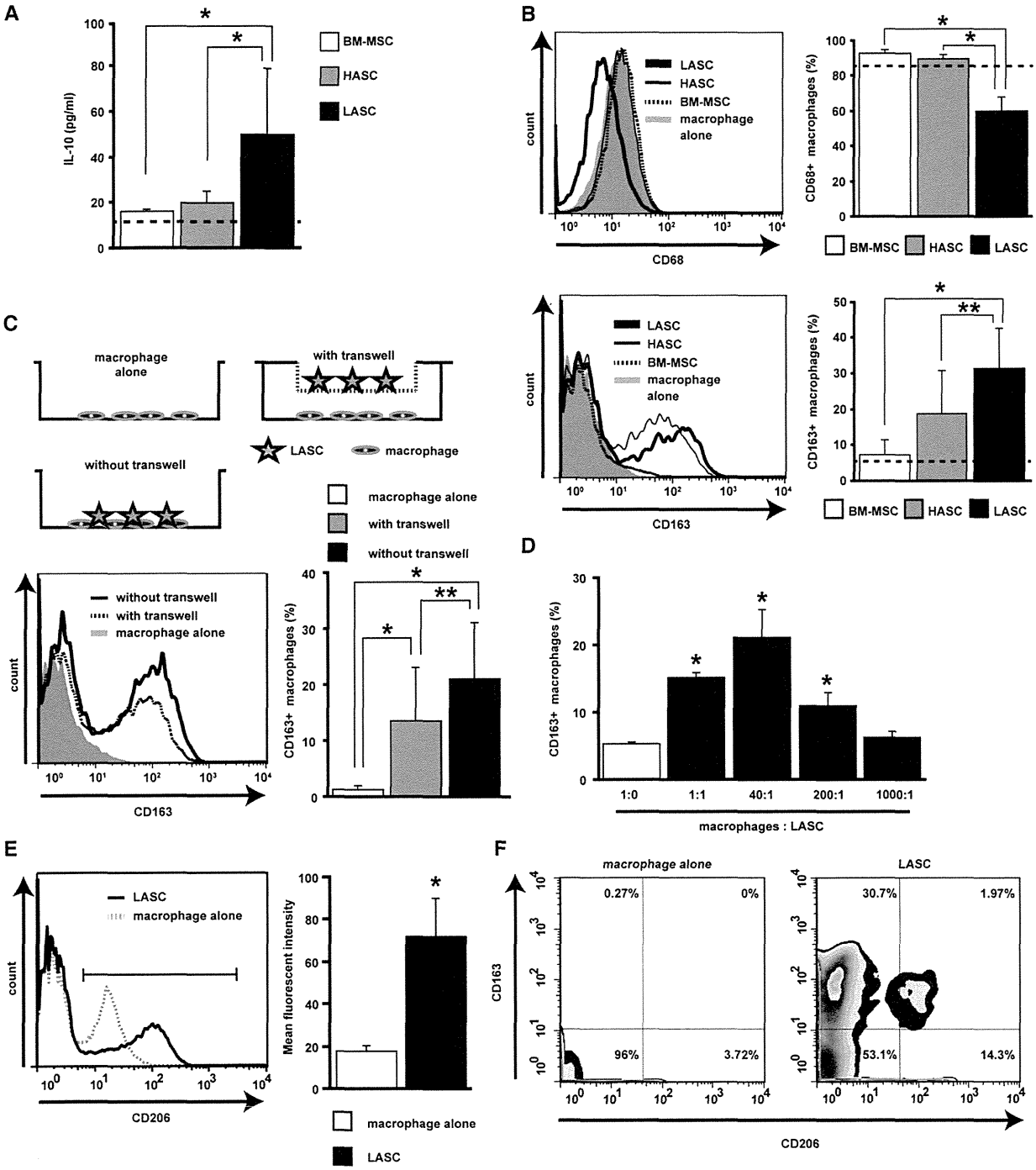

Figure 5. ASC-mediated functional polarization of macrophages into immunoregulatory cells. (A) IL-10 concentration in culture supernatants of peritoneal macrophages cultured for 48 hours with BM-MSCs, HASCs, or LASCs at a 20:1 ratio. Dotted line indicates value in macrophages cultured alone (n=9–13 per group). (B) Expression of CD68 (upper) and CD163 (lower) on peritoneal macrophages cultured with MSCs at a 2:1 ratio is evaluated by flow cytometry. The percentage of $CD68^+$ and $CD163^+$ cells is determined. The population of $CD68^+$ macrophages is significantly reduced and that of $CD163^+$ macrophages is significantly increased when macrophages are cultured with LASCs compared with macrophages cultured with BM-MSCs or HASCs (n=7 per group). Dotted line represents value for macrophages cultured alone (n=7). (C) Macrophage polarization into M2 cells after direct and indirect contact with LASCs. A trans-well plate system prevents direct contact between macrophages and LASCs. Macrophages are cultured on the bottom of the plate and LASCs are cultured in the upper well at a 2:1 ratio. LASC-mediated CD163 expression on macrophages is evaluated

DISCUSSION

Crescent formation is a hallmark of active renal disease and determines the outcome in patients with human GN, including anti-GBM GN, ANCA-associated GN, lupus nephritis, and IgA nephropathy. Although BM-MSC administration has been shown to ameliorate acute tubular injury induced by cisplatin or ischemia reperfusion,[37,38] and subcapsular injection of ASCs in rat kidneys has been shown to reverse folic acid–induced acute tubular damage,[32] the capacity of MSCs to ameliorate glomerular damage has not been demonstrated until this report. Here, we clearly demonstrate the therapeutic superiority of ASCs to BM-MSCs in ameliorating renal damage in a rat crescentic GN model that recapitulates aspects of human anti-GBM GN. In addition, we demonstrate that LASCs in particular attenuate neutrophil, $CD8^+$ T cell, and $CD68^+$ macrophage recruitment during the initial phases of the disease. We also show that LASCs promote the phenotypic switching of glomerular macrophages to immunoregulatory cells during later phases of anti-GBM GN, and that this switching is dependent on LASC-derived PGE2 and IL-6 (Figure 9). Together, these activities of LASCs reduce formation of the glomerular crescents that lead to progressive renal dysfunction and proteinuria.

We showed that intravenous administration of LASCs, HASCs, or BM-MSCs significantly reduces total macrophage infiltration in diseased glomeruli. Phenotypic conversion of macrophages to $CD163^+$ cells in diseased glomeruli was demonstrated in the LASC-treated group, but was less prominent after HASC treatment and was minimal in BM-MSC–treated animals. It is well known that $CD163^+$ macrophages represent anti-inflammatory M2 macrophages,[30,31,39–41] and we and others have clearly demonstrated colocalization of CD163 and cytosolic IL-10 in glomerular macrophages in anti-GBM GN.[28,29] Furthermore, blockage of the angiotensin II receptor or treatment with statins has been shown to attenuate anti-GBM GN, together with augmentation of $CD163^+$ glomerular macrophages.[28,29] In our *in vitro* study, LASC treatment effectively increased the number of $CD163^+$ and $CD206^+$ cells and the level of IL-10 secretion, but only a small population of rat peritoneal macrophages expressed both $CD206^+$ and $CD163^+$ in our coculture system. In addition to our *in vitro* evidence, we found a greater increase in IL-10 secretion in $CD163^+$ cells than in $CD206^+$ cells in diseased glomeruli after LASC transfer. Therefore, we speculate that LASC-mediated conversion of macrophages to IL-10–producing $CD163^+$ cells ameliorates glomerular injury in rat anti-GBM GN. In mice and humans, $CD163^+$ and $CD206^+$ macrophages are classified as anti-inflammatory M2c cells producing IL-10 and profibrotic M2a-like cells, respectively.[30] Interestingly, M2a- or M2c-macrophage transfer has been shown to dramatically attenuate renal injury after mouse adriamycin nephropathy,[42–44] suggesting both M2a and M2c macrophages have renoprotective effects. Considering the above evidence, a precise characterization of the M2 cell subtype induced by LASC treatment and an evaluation of the efficacy of adoptive transfer of $CD163^+$ macrophages is needed for a more complete understanding of the therapeutic significance of LASC-mediated conversion of macrophages into $CD163^+$ cells in anti-GBM GN.

However, it remains unclear whether LASC-induced $CD163^+$ macrophages are directly involved in protecting against anti-GBM GN-induced renal damage. Previous studies involving sepsis models have shown that MSC administration ameliorates tissue injury and neutrophil infiltration into the kidney that are associated with a reduction in the respiratory burst of neutrophils exposed to formyl-Met-leu-Phe-OH (fMLP) *in vitro*.[11,12] With respect to lymphocytes, MSCs have been shown to suppress $CD8^+$ T cell proliferation and cytotoxic activity in cells stimulated with allogeneic peripheral blood lymphocytes, DCs, or phytohemagglutinin *in vitro*.[3,45] In this study, it was clear that LASC treatment reduced glomerular infiltration of $CD8^+$ T cells, neutrophils, and $CD68^+$ macrophages. Therefore, it is possible that LASC-mediated inactivation of neutrophils, $CD8^+$ T cells, and $CD68^+$ macrophages, rather than polarization of $CD163^+$ macrophages is associated with amelioration of anti-GBM GN.

Anti-GBM IgG activates leukocytes and glomerular endothelial cells to elevate local cytokine/chemokine production, and increases expression of adhesion molecules such as intercellular adhesion molecule-1 on leukocytes and endothelial cells in the glomerulus. Subsequent thrombus formation and collapse of capillaries can impair glomerular microcirculation[24,46]; consequently, circulating cells, including leukocytes, platelets, and presumably administrated ASCs as well, tightly adhere to glomerular capillaries and accumulate in diseased glomeruli. We found administered ASCs both in glomerular capillaries and crescents in which $CD163^+$ cells were primarily observed. This proximity to macrophages might be associated with the phenotypic conversion of macrophages in inflamed glomeruli. Administered ASCs were also occasionally observed in the peritubular capillaries of diseased kidneys, but we found no evidence of direct contact between LASCs and $CD163^+$ macrophages in the interstitial capillaries. Whereas interstitial accumulation of $CD68^+$ macrophages

using trans-well plates, and the percentage of $CD163^+$ cells is determined. Macrophages with or without LASCs were subjected to positive and baseline control, respectively (n=7 per group). (D) Analysis of LASC-mediated polarization of macrophages into $CD163^+$ cells under different cell ratios. The percentage of $CD163^+$ cells is determined. (E) CD206 induction on macrophages cocultured with LASCs (left). Mean fluorescence intensity of $CD206^+$ cells (right) is evaluated in the indicated gate. (F) Quadrants and numbers indicate percentage of cells from each gate of $CD163^+$ and/or $CD206^+$ macrophages alone (left) or with LASCs (right) (n=4 per group). All data are mean ± SD. *P<0.01 and **P<0.05 as determined by ANOVA.